Published OnlineFirst November 27, 2017; DOI: 10.1158/1078-0432.CCR-17-2655

Biology of Human Tumors

Clinical Cancer Research

Small-Cell Carcinomas of the Bladder and Lung Are Characterized by a Convergent but Distinct Pathogenesis

Matthew T. Chang[1,2,3], Alexander Penson[1,2], Neil B. Desai[4], Nicholas D. Socci[5,6], Ronglai Shen[2], Venkatraman E. Seshan[2], Ritika Kundra[6], Adam Abeshouse[6], Agnes Viale[6], Eugene K. Cha[7], Xueli Hao[8], Victor E. Reuter[8], Charles M. Rudin[4], Bernard H. Bochner[7], Jonathan E. Rosenberg[4,9], Dean F. Bajorin[4,9], Nikolaus Schultz[2,6], Michael F. Berger[6,8], Gopa Iyer[4,9], David B. Solit[1,4,6,9], Hikmat A. Al-Ahmadie[8], and Barry S. Taylor[1,2,6]

Abstract

Purpose: Small-cell carcinoma of the bladder (SCCB) is a rare and aggressive neuroendocrine tumor with a dismal prognosis and limited treatment options. As SCCB is histologically indistinguishable from small-cell lung cancer, a shared pathogenesis and cell of origin has been proposed. The aim of this study is to determine whether SCCBs arise from a preexisting urothelial carcinoma or share a molecular pathogenesis in common with small-cell lung cancer.

Experimental Design: We performed an integrative analysis of 61 SCCB tumors to identify histology- and organ-specific similarities and differences.

Results: SCCB has a high somatic mutational burden driven predominantly by an APOBEC-mediated mutational process. *TP53*, *RB1*, and *TERT* promoter mutations were present in nearly all samples. Although these events appeared to arise early in all affected tumors and likely reflect an evolutionary branch point that may have driven small-cell lineage differentiation, they were unlikely the founding transforming event, as they were often preceded by diverse and less common driver mutations, many of which are common in bladder urothelial cancers, but not small-cell lung tumors. Most patient tumors (72%) also underwent genome doubling (GD). Although arising at different chronologic points in the evolution of the disease, GD was often preceded by biallelic mutations in *TP53* with retention of two intact copies.

Conclusions: Our findings indicate that small-cell cancers of the bladder and lung have a convergent but distinct pathogenesis, with SCCBs arising from a cell of origin shared with urothelial bladder cancer. *Clin Cancer Res; 24(8); 1965–73. ©2017 AACR.*

See related commentary by Oser and Jänne, p. 1775

Introduction

Bladder cancer is the second most common urinary tract malignancy, responsible for over 165,000 deaths per year worldwide (1). Although urothelial carcinomas predominate, several histologically distinct subtypes are observed, including squamous cell, adenocarcinoma, sarcomatoid, plasmacytoid, and small-cell/neuroendocrine tumors (2). Though histology-specific, pathognomonic genetic lesions exist (3), little is known about the distinguishing genomic features of most bladder cancer histologies. In addition, a comprehensive comparison of the genomic profiles of these histologies as an entry point for understanding their diverse clinical and therapeutic differences is lacking. Small-cell carcinoma of the bladder (SCCB) is a highly aggressive neuroendocrine tumor (4, 5) often associated with a urothelial component. The therapeutic management of SCCB has, to date, been driven by the clinical experience in small-cell lung cancers (6, 7), as these diseases are histologically indistinguishable and share many clinicopathologic characteristics (8). We sought to understand the molecular etiology of SCCB in the context of small-cell lung cancers as well as diverse bladder histologies (2, 3) using genome-wide data from 61 patients compared with comprehensive data from both urothelial tumors and small-cell lung cancers. We identify genetic lesions that arise early in SCCB pathogenesis, and through histology- and organ-specific comparisons, reveal differences in mutational patterns and potential therapeutic targets.

Materials and Methods

Patient samples

All specimens and clinical annotation were obtained from patients providing informed consent and in accordance with

[1]Human Oncology and Pathogenesis Program, Memorial Sloan Kettering Cancer Center, New York, New York. [2]Department of Epidemiology and Biostatistics, Memorial Sloan Kettering Cancer Center, New York, New York. [3]Department of Bioengineering and Therapeutic Sciences, University of California, San Francisco, California. [4]Department of Medicine, Memorial Sloan Kettering Cancer Center, New York, New York. [5]Bioinformatics Core, Memorial Sloan Kettering Cancer Center, New York, New York. [6]Marie-Josée and Henry R. Kravis Center for Molecular Oncology, Memorial Sloan Kettering Cancer Center, New York, New York. [7]Urology Service, Department of Surgery, Memorial Sloan Kettering Cancer Center, New York, New York. [8]Department of Pathology, Memorial Sloan Kettering Cancer Center, New York, New York. [9]Department of Medicine, Weill Cornell Medical College, Cornell University, New York, New York.

Note: Supplementary data for this article are available at Clinical Cancer Research Online (http://clincancerres.aacrjournals.org/).

M.T. Chang and A. Penson contributed equally to this article.

Corresponding Authors: Barry S. Taylor, Memorial Sloan Kettering Cancer Center, 1275 York Avenue, Box 20, New York, NY 10065. Phone: 646-888-3728; Fax: 646-888-3266; E-mail: taylorb@mskcc.org; and Hikmat A. Al-Ahmadie, Department of Pathology, Memorial Sloan Kettering Cancer Center, 1275 York Avenue, New York, NY 10065. E-mail: alahmadh@mskcc.org

doi: 10.1158/1078-0432.CCR-17-2655

Published OnlineFirst November 27, 2017; DOI: 10.1158/1078-0432.CCR-17-2655

Translational Relevance

Beyond their cardinal lesions and distinct pathogenesis, nearly half of small-cell bladder cancers (46%) harbor a potentially therapeutically actionable lesion that may serve as a rationale for clinical hypothesis testing as part of broader early-phase basket studies uniquely suited to the study of such rare tumor types.

institutional review board approval at Memorial Sloan Kettering Cancer Center (MSKCC). Tumor samples were obtained from surgical specimens (either transurethral resection or cystectomy specimens). All tumors were reviewed and histopathologically confirmed to be SCCB (H.A. Al-Ahmadie and X. Hao). Representative formalin-fixed, paraffin-embedded (FFPE) sections (on average, 10 curls of 10 μm) from each sample were selected for analysis. In a subset of cases, macrodissection or microdissection was performed to enrich for tumor content and minimize stromal tissue contamination. Matched normal tissue for germline DNA consisted of blood and/or normal tissues (benign lymph nodes procured at the time of cystectomy). Histologically distinct regions of tumors from patients diagnosed with small-cell bladder cancers presenting with mixed histology disease were further macrodissected and sequenced separately. Immunohistochemistry for retinoblastoma protein (RB) was performed on representative tumor sections using an Rb mouse monoclonal antibody (13A10; Leica Biosystems) on a Ventana Medical Systems DISCOVERY XT platform at 1:50 dilution. Overall, 15 patients underwent whole-exome sequencing (WES), and 2 patients underwent whole-genome sequencing (WGS), both of whom also possessed higher depth of coverage Memorial Sloan Kettering-Integrated Mutation Profiling of Actionable Cancer Targets (MSK-IMPACT) sequencing, and one also had RNA sequencing (RNA-Seq) data. In total, 56 patients had tumor specimens sequenced with MSK-IMPACT using either a 281-gene version ($n = 17$) or a 341-gene version ($n = 40$; 1 patient with two tumors, each of which was sequenced on each assay version). Finally, 12 patients had RNA-Seq of which WES was available for 10 and MSK-IMPACT was available for the remaining 2. In total, 13 patients had multiple spatially or temporally distinct tumor specimens (two or three) sequenced. Full details of the cohort, including clinical data and sequencing platforms used, are available in Supplementary Tables S1 and S2.

Sequencing and analysis

Exome, transcriptome, and targeted sequencing were performed in the Center for Molecular Oncology at MSKCC. DNA extraction was performed from either FFPE or frozen tumors and matched normal specimens with the DNeasy Blood & Tissue Kit (QIAGEN) according to the manufacturer's modified protocol, including the replacement of the AW2 buffer with 80% ethanol. DNA was eluted in nuclease-free water. In total, 13 tumors were subjected to WES, and 500 ng of genomic DNA was captured by hybridization using the SureSelect XT Human All Exon V4 (Agilent Technologies). Samples were prepared according to the manufacturer's instructions. PCR amplification of the libraries was carried out for six cycles in the precapture step and seven cycles postcapture. Samples were barcoded and run on a HiSeq 2500 in a 75-bp paired-end run using the TruSeq SBS Kit v3 (Illumina). The average number of read pairs per sample was 133 and 110 million for tumor and normal samples, respectively, and the average duplication rate was 4.3% and 3.2%. Read processing, alignment, and recalibration as well as somatic mutation (substitutions and small insertions and deletions) calling were performed as previously described (3).

To this exome cohort, we added three additional small-cell bladder cancers that were profiled by The Cancer Genome Atlas (TCGA) but ultimately excluded from the TCGA bladder cancer study cohort (9) due to their non-urothelial histology. Mutations and copy number alterations (CNA) in either 281 or 341 genes were also profiled (in 17 and 41 additional patients, respectively) using a solution-phase hybridization-based exon capture and deep-sequencing assay as previously described (Supplementary Tables S1 and S3; ref. 10). WGS was performed and analyzed, all as previously described (11), on two small-cell bladder tumors and their matched normal specimens, whose DNA was extracted as described above. The results of all sequencing data are available on the publicly accessible cBioPortal for Cancer Genomics (12, 13).

RNA-Seq was performed for 12 small-cell bladder tumors. These transcriptome data were used for fusion detection, mutation cross-validation, and exploring *RB1* dysfunction in presumed *RB1*-wildtype tumors. Briefly, RNA from frozen tissue was extracted using the RNeasy Mini Kit (QIAGEN) according to the manufacturer's instructions. After ribogreen quantification and quality control with an Agilent Technologies Bioanalyzer, 2 μg of total RNA [6.5< RNA integrity number (RIN) <8.1] underwent polyA selection and TruSeq library (TruSeq RNA Sample Prep Kit v2) preparation according to a modified protocol to enhance fusion transcript discovery. Briefly, samples were fragmented for 2 minutes at 94°C before undergoing first-strand and second-strand cDNA synthesis. Libraries were amplified with 10 cycles of PCR and size selected for fragments between 400 and 550 bp with a Pippin Prep instrument (Sage Science). Samples were barcoded and run on a Hiseq 2500 in a 100-bp paired-end run using the TruSeq SBS Kit v3 (Illumina). An average of 32 million paired reads were generated per sample. To these, we added the RNA-Seq data of the three histologically confirmed TCGA small-cell bladder cancers (H.A. Al-Ahmadie), converting aligned reads to FASTQ for merging with sequenced samples before analysis. Transcriptome reads were mapped to the human genome (hg19) using rnaStar ver2.5.0a (14) to map reads genomically and resolve reads across splice junctions. Reads were mapped in a two-pass method (15), the first pass mapping to known annotated junctions from Ensembl, and the second pass is completed on both known and novel junctions found in the first pass. After mapping, expression count matrices were generated from mapped reads using HTSeq ver 0.5.3 using GENCODE ver18 gene models and normalized using DESeq. Candidate fusions were identified using chimerascan 0.4.5, deFuse 0.6.2, and fusioncatcher v0.99.3e. Pairs of genes identified by more than one algorithm were inspected. Subsequent heuristic filtering and manual inspection confirmed all putative fusion calls were false positives.

Retrospective and prospective data

Results from this study cohort (SCCB) were compared with those of four additional cohorts. For urothelial bladder cancer, we combined data from 131 histologically confirmed tumors of the TCGA project (9) with 172 tumors prospectively sequenced as part of an ongoing clinical sequencing initiative at our institution

Published OnlineFirst November 27, 2017; DOI: 10.1158/1078-0432.CCR-17-2655

with the Clinical Laboratory Improvement Amendments (CLIA)–certified MSK-IMPACT assay, which screens 410 cancer-associated genes using the same technology as the targeting sequencing performed above (10). Corresponding aligned read data from WES of the TCGA samples were downloaded from CGHub and reanalyzed with the copy number pipeline described below. For small-cell lung cancers, we combined the somatic mutational data from a recent WGS study of 110 patients (16) with data from 39 tumors prospectively sequenced as described above. Prospective sequencing analysis was performed as previously described and extensively validated for clinical use (10).

Mutational signatures analysis

Mutational signature decomposition analysis (17, 18) was performed for all tumor samples with 10 or more somatic mutations ($n = 61$; ref. 18). From the somatic mutations in an individual tumor sample, we infer contributions from known mutational signatures, which are probability distributions over the nucleotide change and flanking 5′ and 3′ nucleotide context of each mutation. Each mutation in the sample is viewed as a random draw from the following random process: First, a mutational signature is chosen at random according to its contribution, or degree of exposure, and then a mutation type is chosen at random according to that signature. This gives a mixture model, a weighted combination of signatures where the weights are unknown and sum to one, with each weight indicating the proportion of mutations in the sample attributed to that signature. These weights are inferred using an optimization algorithm that maximizes a log-likelihood function derived from this random model. As the APOBEC-mediated mutational process has been attributed to two distinct signatures (signatures 2 and 13; ref. 17), for visualization purposes we show the sum of the fractions of both signatures.

Copy number, clonality, and evolutionary analyses

We determined total, allele-specific, and integer DNA copy number genome wide using the FACETS algorithm (19) in all tumors ($n = 81$) independent of sequencing platform (targeted, exome, or genome). Briefly, FACETS simultaneously segments total and allele-specific DNA copy number from the coverage and genotypes of polymorphic SNPs genome wide. Allele-specific segmentation is based on the log odds ratio of allele fractions at SNPs identified as heterozygous in the normal sample. A fit is applied to the resulting segments, identifying in each sample the (i) log ratio corresponding to diploidy, (ii) purity, and (iii) average ploidy. Major and minor integer copy number is then assigned to each segment by maximum likelihood. Allelic imbalance (including tumor-specific loss-of-heterozygosity) is determined from a change in the zygosity of heterozygous SNPs. We then defined the presence of genome doubling (GD) in samples for which the majority of the genome (≥50%) contains multiple copies from the same parent/allele. Gene-level copy number (Supplementary Table S4) was assigned from spanning segments of integer copy number data in each tumor. Homozygous deletion was determined from regions of total copy number of zero. Amplifications were those regions of total integer copy number greater than 5 or 6 in diploid and GD cases, respectively. Partial deletions (with intragenic breakpoints) were called whereas partial amplifications were not. This same FACETS-based analytical pipeline was run on all retrospective and prospective cohorts (including both targeted and WES data) to allow for direct comparison of gene-level copy number calls.

The purity and integer copy number results from FACETS analysis, along with coverage levels and allele frequencies, were used to estimate the fraction of cancer cells harboring each mutation [cancer cell fraction (CCF)] in all evaluable specimens ($n = 77$). For mutations in regions of genomic gain, two CCFs were calculated, assuming the minimum and maximum possible number of copies (20). For each CCF, confidence intervals were estimated as the full width half maximum of the posterior probability distribution (21). The timing of emergence of GD relative to somatic mutations was estimated by applying a Gaussian mixture model to the allele fractions of somatic mutations in genomic regions of balanced tetraploidy in 10 tumors for which a sufficient number of such mutations were present (≥20). Mutations that could be confidently assigned membership in the mixture model were assumed to have arisen before or after GD. The number of copies of each mutation per cancer cell, and, therefore, timing relative to GD, was estimated when there was sufficient separation between component allele fraction distributions per sample. In general, somatic CNAs can also be timed, however, the burden of CNAs in small-cell bladder cancer is so high that often, the majority of a genome has been affected by multiple independent CNA events. As a result, only a few events can be timed unambiguously.

In the 2 patients in our cohort with mixed-histology disease, histology-specific regions were macrodissected, so we, therefore, expected that a minimal amount of cross-contamination among the populations may be present. We corrected for this analytically in the following manner: As the estimated tumor purity was similar, for all mutations shared between the two cell populations in regions that lacked CNAs, we determined the mode of the distribution of the ratio of allele frequencies between the small-cell and other histologic populations. Mutations in the non–small-cell population with allele frequencies less than or equal to the positive full width at half maximum of this distribution of ratios between the two populations were considered to be arising from a minor contaminating population of small cell present in the second histology and were excluded from comparisons.

Data availability

All somatic mutational calls and CNAs along with accompanying clinical data are available for analysis and visualization in the cBioPortal for Cancer Genomics (http://cbioportal.org/). Raw sequencing data have been deposited in the Database of Genotypes and Phenotypes (dbGaP; http://www.ncbi.nlm.nih.gov/gap/).

Results

We analyzed 87 tumor and matched normal specimens from 61 patients with SCCB with a combination of whole-exome, -genome, and -transcriptome sequencing along with targeted deep sequencing of hundreds of key cancer-associated genes (see "Materials and Methods" and Supplementary Tables S1 and S3). This cohort is comprised predominantly of men (79%) with largely muscle-invasive (stage ≥2) disease at diagnosis (89%), who received chemotherapy and had a median overall survival of 45 months (95% confidence interval, 31–60; Supplementary Table S2). To explore bladder histology-, cell lineage-, and organ-specific differences, we compared these results with

Published OnlineFirst November 27, 2017; DOI: 10.1158/1078-0432.CCR-17-2655

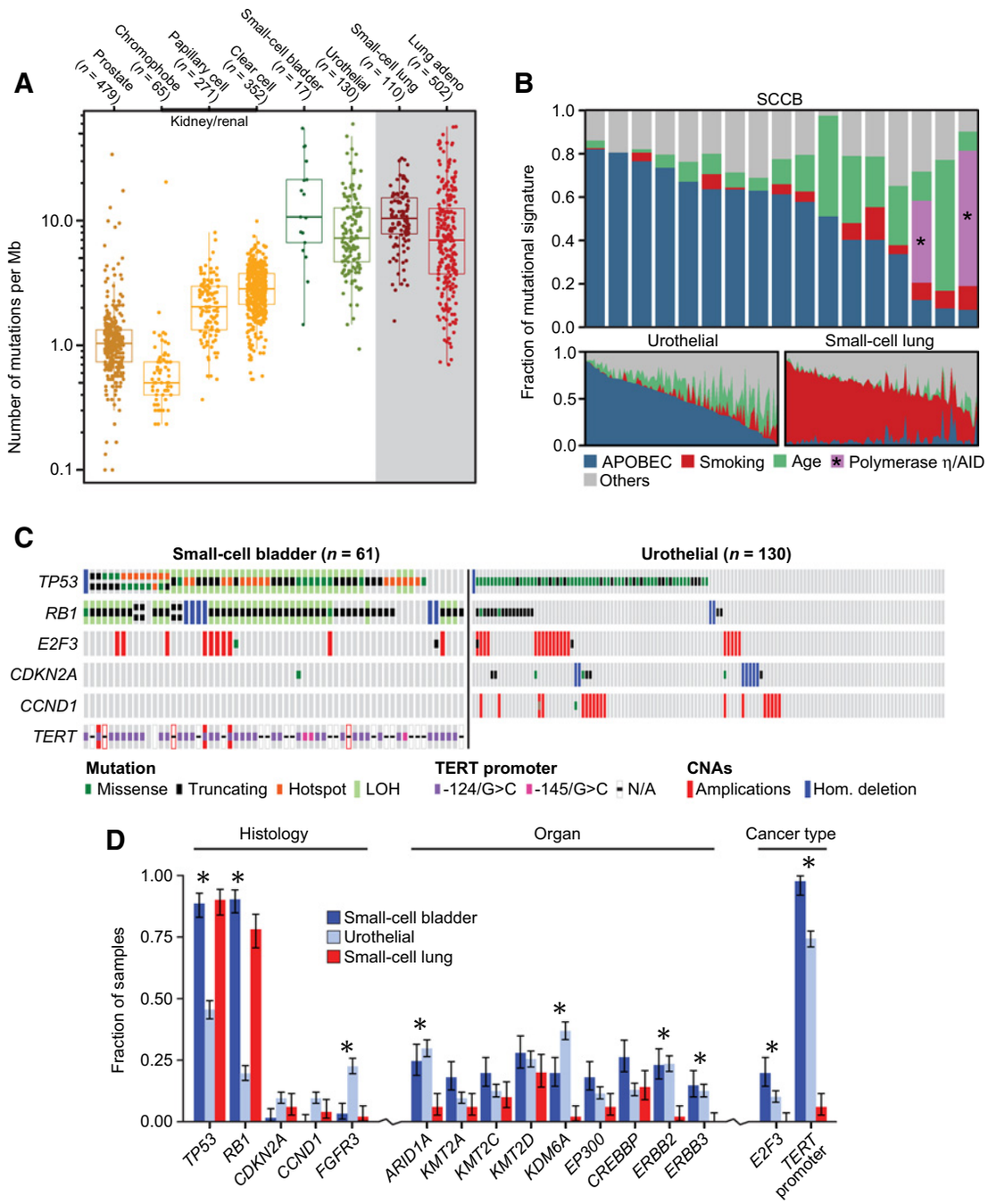

Figure 1.

Mutational burden of SCCB. **A,** The somatic mutational burden of SCCBs, other genitourinary cancers, and both pulmonary adenocarcinomas (adeno) and small-cell carcinomas. Box represents interquartile range (IQR); upper whisker extends from hinge to largest value ≤1.5x IQR. **B,** Mutational signatures in patients with SCCB with WES or WGS data (includes three TCGA small-cell bladder samples, see "Materials and Methods"), urothelial tumors, and small cell lung cancers (bottom). Patients 6 and 23 possessed a polymerase η-associated activation-induced cytidine deaminase (AID) mutational signature, as indicated. **C,** Pattern of lesions in *TP53, RB1*, the *TERT* promoter, and other effectors of cell-cycle regulation in SCCBs and urothelial carcinomas (as labeled, urothelial inferred from TCGA data). **D,** Commonly mutated genes in SCCB, urothelial carcinomas, and small-cell lung cancers (dark blue, light blue, and red, respectively) are grouped on the basis of their alteration frequency being predominantly associated with either histology, organ, or cancer-type alteration patterns (*, nominal *P* value < 0.05; Fisher exact test, error bars represent one standard deviation using the binomial distribution). Hom., homozygous; LOH, loss of heterozygosity; N/A, not available.

Published OnlineFirst November 27, 2017; DOI: 10.1158/1078-0432.CCR-17-2655

genomic data from 452 retrospectively and prospectively sequenced high-grade urothelial bladder (9, 22) or small-cell lung cancers (ref. 23; 303 and 149, respectively; see "Materials and Methods"). WES and/or WGS of the tumor and matched normal specimens from 17 patients revealed a high somatic mutational burden [median of 10.7 mutations per million bases (Mb) sequenced] that was significantly greater than other genitourinary cancers (Fig. 1A). Despite the prevalence of a past history of smoking (73% were current or former smokers; Supplementary Table S2), mutational signature decomposition analysis (17) in these patients revealed that APOBEC rather than tobacco-associated mutagenesis predominated. Indeed, 95% of these patients harbored evidence of an APOBEC-mediated mutational process that accounted for a median of 60 ± 23.7% of all somatic mutations in each patient (Fig. 1B). This APOBEC-driven mutational signature (predominantly C>G or C>T mutations at the TCW trinucleotide context) was observed to a lesser degree in bladder urothelial carcinoma but was largely absent from small-cell lung cancers despite a shared risk factor of past smoking history in all three cancer types (refs. 4, 23–25; Fig. 1B, bottom). Endogenous mutational processes other than APOBEC were present in a subset of samples including 2 patients with a mutational signature associated with polymerase η/activation-induced cytidine deaminase (AID) defects. Taken together, this suggests that risk of smoking-associated bladder cancers is driven by a pathogenic mechanism different than the mutagenesis observed in small-cell lung cancers.

TP53 and *RB1* were the most frequently altered genes in SCCB, each arising in 90% of patients (Fig. 1C; Supplementary Tables S5 and S6). Mutations in these genes co-occurred in 80% of all tumors, a pattern that is consistent with small-cell lung cancers (16) and underscores the importance of G_1- to S-phase cell-cycle dysregulation in small-cell cancers independent of their organ of origin. Moreover, transcriptome sequencing in 12 patients, although not identifying recurrent gene fusions in SCCBs, did reveal loss of *RB1* expression in an SCCB that lacked an *RB1* mutation. We confirmed with immunohistochemistry in 2 additional *RB1*–wild-type patients that these tumors did not express RB (Supplementary Fig. S1), suggesting the presence of occult lesions or epigenetic silencing as the basis for *RB1* inactivation in such cases. SCCBs also had a much higher rate of biallelic mutation in these genes compared with urothelial tumors (Supplementary Fig. S2). However, 12% of histologically confirmed urothelial bladder cancers also harbored co-occurring alterations in *TP53* and *RB1* (9), suggesting that mutations in one or both of these genes are necessary but not sufficient for the development of the small-cell phenotype. Targeted sequencing of 341 key cancer-associated genes at high depth of coverage in 46 additional SCCBs confirmed these coincident mutations and further revealed that 95% of SCCBs harbor *TERT* promoter mutations that are also present less frequently in 70% of urothelial tumors (prospective cohort; see "Materials and Methods;" $P < 1.6 \times 10^{-4}$, Fisher exact test), but that are absent from other small-cell cancer types, including small-cell lung cancers (26). Combining the unbiased and targeted sequencing cohorts, we found that recurrent mutations in diverse epigenetic modifiers (*KDM6A*, *ARID1A*, *CREBBP*, *EP300*, and *KMT2A/C/D*) were present in most patients with SCCB (74%, $n = 45$ of 61), a mutational frequency of these genes similar to that observed in urothelial carcinoma. Mutations in these chromatin-modifying genes were, however, uncommon in small-cell lung cancers ($P < 10^{-6}$, Fisher exact test; Fig. 1D), indicating that SCCB likely arises from a urothelial carcinoma precursor and has a pathogenesis distinct from that of small-cell lung cancers.

Like the genomes of small-cell lung cancer, SCCB genomes were complex, although in distinct ways (Supplementary Fig. S3). On average, 63% of the SCCB genome harbored DNA CNAs, similar to urothelial carcinomas with *TP53* mutations but higher than other epithelial tumors. Focal homozygous and heterozygous deletions of the *RB1* and *TP53* loci were the most frequent CNAs, contributing to biallelic alterations. Focal *CDKN2A* deletions and *CCND1* amplifications, although common in urothelial carcinoma, were absent from SCCB ($P = 0.02$ and 0.0005, Fisher exact test). Organ-specific *E2F3* focal amplifications were present in 17% of SCCBs, a frequency similar to that observed in urothelial carcinoma but significantly higher than in small-cell lung cancers (Fig. 1D). Although many of these complex amplicons also span *SOX4*, another previously hypothesized target of this CNA, WGS resolved the structure of one such event in an affected patient, indicating that *E2F3* is the likely target (Supplementary Fig. S4). Moreover, the presence of *E2F3* amplifications in *RB1*-null tumors indicates that the former may confer an additional growth advantage or that these effectors have organ- rather than cell-type–specific nonredundant roles despite their shared regulation of the G_1- to S-phase transition of the cell cycle. Beyond focal CNAs, recurrent broad gains and losses were common, but the frequent 3p losses present in small-cell lung cancers were largely absent in SCCB. Notably, although 5p gains were the most common broad CNA in SCCB (10%), these events did not exclusively target the mutant allele of the *TERT* promoter (5p15). Indeed, 5p genomic gains targeted the wild-type allele of *TERT* in four tumors, indicating that there is a selective pressure for 5p gains beyond elevating expression of mutant *TERT*, perhaps targeting another oncogene on the chromosome arm.

Given the chromosomal instability in SCCB, we investigated the presence of GD, which has been previously associated with poor prognosis in individual cancer types (27). Using inferences of ploidy from genome-wide allele-specific copy number (Fig. 2A), we identified GD in 72% of 58 evaluable tumors (Fig. 2B; Supplementary Table S7), a frequency similar to that observed in urothelial carcinoma, not otherwise specified (NOS) tumors (28). Whereas GD has been associated with *TP53* mutations in other tumor types (27, 28), GD was more common in SCCBs with missense rather than loss-of-function *TP53* mutations (nonsense, frameshift, splice site, and homozygous deletions; $P < 10^{-4}$, Fisher exact test; Fig. 2C). Moreover, there appeared to be selection for biallelic alteration of *TP53* missense-mutant GD-positive tumors. Among tumors with *TP53* biallelic mutation, a single mutation followed by copy-neutral loss-of-heterozygosity (CN-LOH) predominated (Fig. 2C; Supplementary Fig. S5). Notably, in GD-positive tumors from 3 patients in which the two independent *TP53* mutations could be phased, we confirmed they were present *in trans* (Fig. 2D).

To better understand how such cardinal events and GD evolved in SCCB, we sought to time the emergence of specific genomic alterations in the chronology of disease pathogenesis from individual tumor specimens. In 10 tumors harboring sufficient somatic mutations (≥20) in regions of balanced tetraploidy for the timing analysis, we found that GD arose at various points in molecular time relative to other somatic mutations (Fig. 3A). The coincident *RB1*, *TP53*, and *TERT* promoter mutations, however, arose before GD in all tumors, emphasizing their early role in SCCB pathogenesis. In some patients, typified by the paired

Published OnlineFirst November 27, 2017; DOI: 10.1158/1078-0432.CCR-17-2655

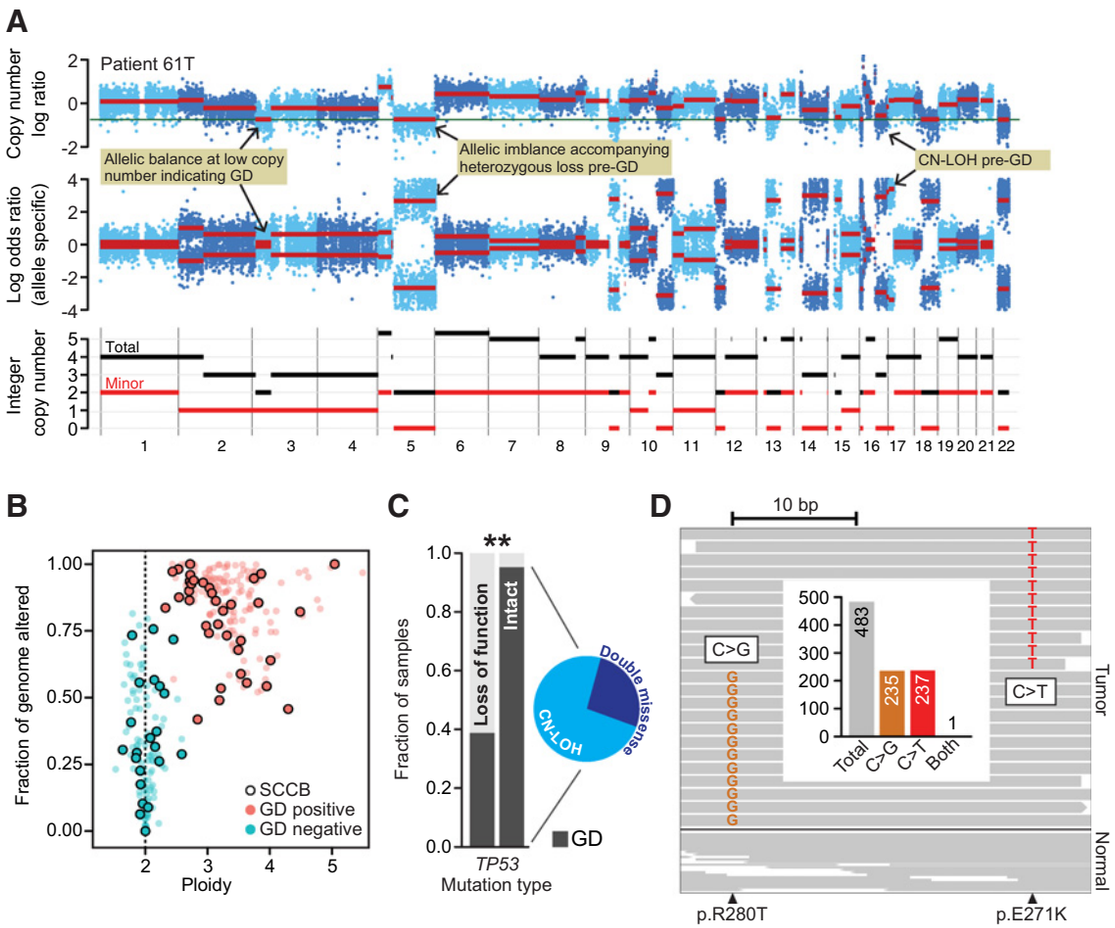

Figure 2.

GD as a function of *TP53* aberrations. **A,** Total, allele-specific, and integer copy number segmentation inferred from WES (chromosomes 1–22; top, middle, bottom) of a representative SCCB genome is shown (patient 61T). Hallmark lesions are indicated (yellow). **B,** The overall burden of CNAs as a function of tumor ploidy in both SCCBs and urothelial carcinomas (points are individual tumors, and SCCBs are those with black border). GD-positive tumors are in red. GD-positive tumors have both higher ploidy and elevated levels of CNAs genome wide. **C,** GD as a function of *TP53* mutational and zygosity status (biallelic missense, with inset representing underlying mechanism; *, $P < 10^{-4}$, Fisher exact test). **D,** A representative tumor possessing two independent *TP53* mutations (patient 70, R280T and E271K) that could be phased; reads spanning both mutant sites indicate that the mutations were *in trans*. Inset, targeting sequencing coverage of reads spanning both mutations is shown, indicating the near absence of reads harboring both mutant alleles.

primary and metastatic tumors of patient 37, only a small minority of the total somatic mutational burden (<5%) arose before GD, indicating GD itself was an early event, perhaps arising shortly after *TP53* alteration(s), whereas in other patients, most somatic mutations, including the cardinal coincident lesions, arose before GD, as was the case for patients 7 and 61. Notably, even the dominant mutational process varied with time. For instance, the APOBEC-associated mutational signature so pervasive in SCCBs was observed only after GD in patient 59, despite 28% of its somatic mutational burden arising before GD (Fig. 3B). In other patients, the APOBEC-associated mutational process produced most somatic mutations early but ebbed as the tumor evolved after GD. Integrating these chronologic analyses in a representative SCCB (patient 61), we found that the cardinal *TP53*, *RB1*, and *TERT* promoter mutations all arose very early in molecular time. *RB1* and *PTEN* biallelic inactivation evolved from truncating mutations after which heterozygous losses targeting the wild-type allele occurred. Conversely, a *TP53* E285K missense mutation was followed by CN-LOH resulting in two copies of the mutant allele after which GD arose, increasing the mutant allele burden of all four of these genes (Fig. 3C). Although most other predominantly APOBEC-associated somatic mutations arose before GD, indicating it was a later event in this patient, several broad CNAs appeared both before and after GD. In the patient in whom we profiled a primary diagnostic tumor and matched adrenal metastasis, the vast majority of somatic mutations were clonal in both, indicating that both tumors emerged from a shared antecedent clone after which linear clonal evolution was evident with only a few metastasis-specific CNAs arising late.

To explore how cardinal events such as *RB1*, *TP53*, and *TERT* promoter mutations arise and contribute to the conversion of a preceding urothelial carcinoma to predominant small-cell histology, we sampled and deeply sequenced histologically distinct regions of tumors with clear and spatially separated regions of both small-cell and urothelial carcinoma, NOS from the same patients. By comparing the mutations common among, or specific

Published OnlineFirst November 27, 2017; DOI: 10.1158/1078-0432.CCR-17-2655

to, multiple histologically distinct regions of mixed-histology tumors presumably originating from a single common ancestor, we can draw inferences on the timing of their emergence and their phylogenetic origins. In 2 such patients, each with two histologically distinct tumor specimens sequenced by MSK-IMPACT, a pattern of branching evolution was apparent. The branch point, defined by specific somatic mutations, represented cellular differentiation between histologies. In both illustrative cases, one or more truncal mutations were clonal in both cell populations. In 1 patient, a single *CREBBP* L1458* nonsense mutation was clonal in both the small-cell and urothelial cell populations (Fig. 3D), whereas *RB1* and *TP53* mutations were

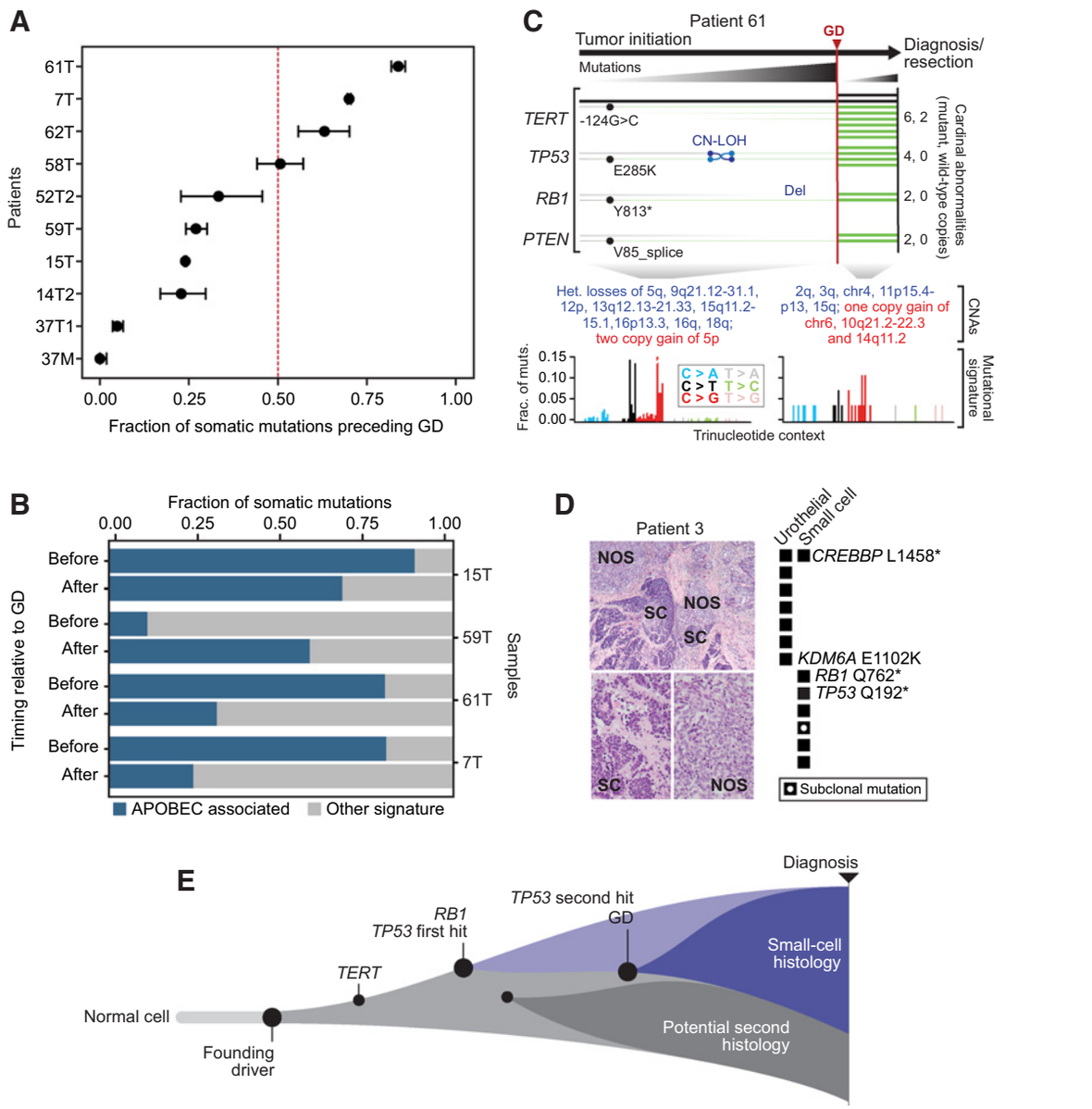

Figure 3.

Heterogeneous evolutionary histories. **A,** GD can arise at different points in the chronology of tumor development, as indicated by the fraction of somatic mutations present at diagnosis that arose before and after GD (error bars represent one standard deviation using the binomial distribution; 10 patients shown are those with ≥20 somatic mutations in regions of balanced tetraploidy). **B,** Although in some tumors, APOBEC-associated mutagenesis is constant before and after GD, in others it either accelerates or ebbs after a GD, indicating that the pressure of a given mutagenic process is not constant in SCCB evolution. **C,** Integrated analysis of mutational event timing in a typical SCCB (patient 61) indicates that multiple mutant copies of cardinal lesions are present after a late GD event that is preceded by most the APOBEC-induced somatic mutational burden. **D,** Coincident urothelial [not otherwise specified (NOS)] and small-cell (SC) histologies from a single patient with mixed-histology disease (left) and the corresponding lesion-specific somatic mutations (right). **E,** Schematic of the evolution of SCCBs in which a founding lesion that initiates cellular transformation precedes the cardinal *RB1*/*TP53* lesions that define a branch point of the small-cell histology that may or may not coexist with a second minor population of a distinct histology with its own lesions. Del, deletion; Het., heterozygous.

Published OnlineFirst November 27, 2017; DOI: 10.1158/1078-0432.CCR-17-2655

present and clonal in only the small-cell component. Conversely, several mutations including *KDM6A* E1102K were present exclusively in the urothelial component, a finding that is consistent with the increased frequency of *KDM6A* mutations in urothelial carcinoma overall compared with SCCB (Fig. 1D). In the other patient, both a *TERT* promoter mutation (-145/C>T) and a *PIK3CA* Q546P hotspot mutation, along with several others, were clonal in both the small-cell and urothelial (papillary) tumor components arising before the cellular differentiation program that defined the two histologies (Supplementary Fig. S6). On the other hand, the small-cell component again exclusively possessed *RB1* and *TP53* mutations, whereas the papillary population possessed a clonal activating *ERBB2* L755S mutation. These results reaffirm the nearly obligate emergence of *RB1* and *TP53* mutations in SCCB but also indicate that these two cardinal events are not the founder mutations necessary for initial transformation and clonal outgrowth of a histologically distinct bladder tumor cell population (Fig. 3E).

Despite the evolutionary heterogeneity of SCCB, most driver mutations of potential clinical actionability were clonal at diagnosis. Exploring the landscape of potentially actionable lesions in SCCB, we found that 46% of patients ($n = 28$ of 61) harbored a lesion of potential therapeutic significance, defined as either an FDA-approved or National Comprehensive Cancer Network (NCCN) compendium–listed biomarker or prior clinical evidence associating it as a biomarker of drug response in this or another indication (Supplementary Fig. S7). In total, 13% of patients (8 of 61) harbored mutations in *PIK3CA* (Supplementary Fig. S7A). Unlike in urothelial carcinoma, SCCBs lack *ERBB2* amplifications (9, 29), but 14 patients harbored likely activating *ERBB2* mutations including hotspot mutations in both the extracellular (S310) and kinase domains (L755; Supplementary Fig. S7B). Among other RTKs, *ERBB3* mutations affected 15% of patients. *FGFR3* hotspot mutations (S249C) were much less common in SCCB than in UC, likely owing to their mutual exclusivity with *RB1* loss, reaffirming the highly RB1-dependent G_1–S checkpoint dysfunction in these tumors. Beyond mutations in *ERCC2*, which correlate with sensitivity to platinum-based therapy in muscle-invasive bladder cancers (30), there were also mutations in other effectors of DNA repair signaling (Supplementary Fig. S7C). Overall, the presence of therapeutically actionable lesions within SCCBs revealed specific clinical hypotheses that can be tested as part of broader early-phase basket studies that are uniquely suited to study such rare tumor types.

Discussion

Our findings indicate that SCCBs and small-cell carcinomas of the lung have a convergent but distinct pathogenesis. Consistent with small-cell lung cancer, we observed obligate, likely early-arising lesions in *RB1* and *TP53*. We also identified bladder-specific mutations in the *TERT* promoter and in chromatin-modifying genes, among others. A substantial subset of *TP53* mutations were biallelic missense rather than loss of function, a setting in which GD arose preferentially, suggesting that GD is more strongly associated with *TP53* neomorphism rather than conventional loss of function in SCCB. Also, although evolutionarily diverse, we demonstrated that there are truncal mutations in tumors with mixed histology (31), but histology-specific lesions in *RB1* and *TP53* determine the small-cell phenotype and appear to arise early in molecular time, likely shortly after the founding driver. This indicates that small-cell and urothelial bladder cancers have a shared cellular origin, with the former representing a dedifferentiation from urothelial carcinoma quite unlike small-cell histologies in other organ types (Fig. 3E; refs. 32, 33). Of course, a small percentage of urothelial carcinomas also harbor alterations in *RB1* and *TP53*, which can be detected in even noninvasive precursor lesions (unpublished data). Therefore, although these lesions are necessary, they alone are likely insufficient to drive small-cell differentiation. Moreover, unlike in prostate cancers progressing on antiandrogen therapy (34), transdifferentiation in bladder cancers has been difficult to identify. Therefore, future studies should explore whether epigenomic or transcriptional events interact with the loss of *RB1* and *TP53* to confer the small-cell phenotype. Taken together, however, these findings suggest that the undifferentiated neuroendocrine features present in small-cell carcinoma are likely associated with the specific alterations present in the affected cell rather than prior mutagen exposure, tissue of origin, or mutational burden. Overall, aside from *RB1* and *TP53* alterations, genomic alterations present in SCCB more closely resemble urothelial carcinoma than small-cell lung cancers, indicating that most alterations contribute to oncogenesis in an organ-specific manner rather than a cell type–specific manner.

Disclosure of Potential Conflicts of Interest

C.M. Rudin is a consultant/advisory board member for Abbvie, AstraZeneca, Bristol-Myers Squibb, Harpoon, and SeattleGenetics. D.B. Solit is a consultant/advisory board member for Loxo Oncology and Pfizer. H.A. Al-Ahmadie is a consultant/advisory board member for Bristol-Myers Squibb and EMD Serono, Inc. No potential conflicts of interest were disclosed by the other authors.

Authors' Contributions

Conception and design: E.K. Cha, G. Iyer, D.B. Solit, H.A. Al-Ahmadie, B.S. Taylor

Development of methodology: M.T. Chang, A. Penson, A. Abeshouse, D.B. Solit, B.S. Taylor

Acquisition of data (provided animals, acquired and managed patients, provided facilities, etc.): N.B. Desai, A. Viale, E.K. Cha, X. Hao, V.E. Reuter, B.H. Bochner, J.E. Rosenberg, D.F. Bajorin, G. Iyer, D.B. Solit, H.A. Al-Ahmadie

Analysis and interpretation of data (e.g., statistical analysis, biostatistics, computational analysis): M.T. Chang, A. Penson, N.D. Socci, R. Shen, V.E. Seshan, J.E. Rosenberg, N. Schultz, M.F. Berger, G. Iyer, D.B. Solit, H.A. Al-Ahmadie, B.S. Taylor

Writing, review, and/or revision of the manuscript: M.T. Chang, A. Penson, E.K. Cha, C.M. Rudin, B.H. Bochner, J.E. Rosenberg, D.F. Bajorin, G. Iyer, D.B. Solit, H.A. Al-Ahmadie, B.S. Taylor

Administrative, technical, or material support (i.e., reporting or organizing data, constructing databases): M.T. Chang, N.B. Desai, R. Kundra, D.B. Solit, B.S. Taylor

Study supervision: D.B. Solit, H.A. Al-Ahmadie, B.S. Taylor

Acknowledgments

The authors would like to thank the members of the Marie-Josée and Henry R. Kravis Center for Molecular Oncology for their assistance. This work was supported in part through NIH awards T32 GM007175 (to M.T. Chang), P30 CA008748, UL1 TR024996, and R01 CA204749 (to B.S. Taylor); the Sontag Foundation (to B.S. Taylor); the Robertson Foundation and Prostate Cancer Foundation (to N. Schultz and B.S. Taylor); and Cycle for Survival (to D.B. Solit, H.A. Al-Ahmadie, and B.S. Taylor).

The costs of publication of this article were defrayed in part by the payment of page charges. This article must therefore be hereby marked *advertisement* in accordance with 18 U.S.C. Section 1734 solely to indicate this fact.

Received September 13, 2017; revised October 23, 2017; accepted November 22, 2017; published first November 27, 2017.

Published OnlineFirst November 27, 2017; DOI: 10.1158/1078-0432.CCR-17-2655

References

1. Torre LA, Bray F, Siegel RL, Ferlay J, Lortet-Tieulent J, Jemal A. Global cancer statistics, 2012. CA Cancer J Clin 2015;65:87–108.
2. Knowles MA, Hurst CD. Molecular biology of bladder cancer: new insights into pathogenesis and clinical diversity. Nat Rev Cancer 2015;15:25–41.
3. Al-Ahmadie HA, Iyer G, Lee BH, Scott SN, Mehra R, Bagrodia A, et al. Frequent somatic CDH1 loss-of-function mutations in plasmacytoid variant bladder cancer. Nat Genet 2016;48:356–8.
4. Cheng L, Pan CX, Yang XJ, Lopez-Beltran A, MacLennan GT, Lin H, et al. Small cell carcinoma of the urinary bladder: a clinicopathologic analysis of 64 patients. Cancer 2004;101:957–62.
5. Quek ML, Nichols PW, Yamzon J, Daneshmand S, Miranda G, Cai J, et al. Radical cystectomy for primary neuroendocrine tumors of the bladder: the university of southern california experience. J Urol 2005;174:93–6.
6. Mukesh M, Cook N, Hollingdale AE, Ainsworth NL, Russell SG. Small cell carcinoma of the urinary bladder: a 15-year retrospective review of treatment and survival in the Anglian Cancer Network. BJU Int 2009; 103:747–52.
7. Siefker-Radtke AO, Kamat AM, Grossman HB, Williams DL, Qiao W, Thall PF, et al. Phase II clinical trial of neoadjuvant alternating doublet chemotherapy with ifosfamide/doxorubicin and etoposide/cisplatin in small-cell urothelial cancer. J Clin Oncol 2009;27:2592–7.
8. Abbas F, Civantos F, Benedetto P, Soloway MS. Small-cell carcinoma of the bladder and prostate. Urology 1995;46:617–30.
9. Cancer Genome Atlas Research Network. Comprehensive molecular characterization of urothelial bladder carcinoma. Nature 2014;507: 315–22.
10. Cheng DT, Mitchell TN, Zehir A, Shah RH, Benayed R, Syed A, et al. Memorial sloan kettering-integrated mutation profiling of actionable cancer targets (MSK-IMPACT): a hybridization capture-based next-generation sequencing clinical assay for solid tumor molecular oncology. J Mol Diagn 2015;17:251–64.
11. Al-Ahmadie H, Iyer G, Hohl M, Asthana S, Inagaki A, Schultz N, et al. Synthetic lethality in ATM-deficient RAD50-mutant tumors underlies outlier response to cancer therapy. Cancer Discov 2014;4:1014–21.
12. Cerami E, Gao J, Dogrusoz U, Gross BE, Sumer SO, Aksoy BA, et al. The cBio cancer genomics portal: an open platform for exploring multidimensional cancer genomics data. Cancer Discov 2012;2:401–4.
13. Gao J, Aksoy BA, Dogrusoz U, Dresdner G, Gross B, Sumer SO, et al. Integrative analysis of complex cancer genomics and clinical profiles using the cBioPortal. Sci Signal 2013;6:pl1.
14. Dobin A, Davis CA, Schlesinger F, Drenkow J, Zaleski C, Jha S, et al. STAR: ultrafast universal RNA-seq aligner. Bioinformatics 2013;29:15–21.
15. Engstrom PG, Steijger T, Sipos B, Grant GR, Kahles A, Ratsch G, et al. Systematic evaluation of spliced alignment programs for RNA-seq data. Nat Methods 2013;10:1185–91.
16. George J, Lim JS, Jang SJ, Cun Y, Ozretic L, Kong G, et al. Comprehensive genomic profiles of small cell lung cancer. Nature 2015;524:47–53.
17. Alexandrov LB, Nik-Zainal S, Wedge DC, Aparicio SA, Behjati S, Biankin AV, et al. Signatures of mutational processes in human cancer. Nature 2013; 500:415–21.
18. Alexandrov LB, Nik-Zainal S, Wedge DC, Campbell PJ, Stratton MR. Deciphering signatures of mutational processes operative in human cancer. Cell Rep 2013;3:246–59.
19. Shen R, Seshan VE. FACETS: allele-specific copy number and clonal heterogeneity analysis tool for high-throughput DNA sequencing. Nucleic Acids Res 2016;44:e131.
20. Greenman CD, Pleasance ED, Newman S, Yang F, Fu B, Nik-Zainal S, et al. Estimation of rearrangement phylogeny for cancer genomes. Genome Res 2012;22:346–61.
21. McGranahan N, Favero F, de Bruin EC, Birkbak NJ, Szallasi Z, Swanton C. Clonal status of actionable driver events and the timing of mutational processes in cancer evolution. Sci Transl Med 2015;7:283ra54.
22. Kim PH, Cha EK, Sfakianos JP, Iyer G, Zabor EC, Scott SN, et al. Genomic predictors of survival in patients with high-grade urothelial carcinoma of the bladder. Eur Urol 2015;67:198–201.
23. Cumberbatch MG, Rota M, Catto JW, La Vecchia C. The role of tobacco smoke in bladder and kidney carcinogenesis: a comparison of exposures and meta-analysis of incidence and mortality risks. Eur Urol 2016; 70:458–66.
24. Freedman ND, Silverman DT, Hollenbeck AR, Schatzkin A, Abnet CC. Association between smoking and risk of bladder cancer among men and women. JAMA 2011;306:737–45.
25. Kenfield SA, Wei EK, Stampfer MJ, Rosner BA, Colditz GA. Comparison of aspects of smoking among the four histological types of lung cancer. Tob Control 2008;17:198–204.
26. Zheng X, Zhuge J, Bezerra SM, Faraj SF, Munari E, Fallon JT III, et al. High frequency of TERT promoter mutation in small cell carcinoma of bladder, but not in small cell carcinoma of other origins. J Hematol Oncol 2014;7:47.
27. Dewhurst SM, McGranahan N, Burrell RA, Rowan AJ, Gronroos E, Endesfelder D, et al. Tolerance of whole-genome doubling propagates chromosomal instability and accelerates cancer genome evolution. Cancer Discov 2014;4:175–85.
28. Zack TI, Schumacher SE, Carter SL, Cherniack AD, Saksena G, Tabak B, et al. Pan-cancer patterns of somatic copy number alteration. Nat Genet 2013; 45:1134–40.
29. Iyer G, Al-Ahmadie H, Schultz N, Hanrahan AJ, Ostrovnaya I, Balar AV, et al. Prevalence and co-occurrence of actionable genomic alterations in high-grade bladder cancer. J Clin Oncol 2013;31:3133–40.
30. Van Allen EM, Mouw KW, Kim P, Iyer G, Wagle N, Al-Ahmadie H, et al. Somatic ERCC2 mutations correlate with cisplatin sensitivity in muscle-invasive urothelial carcinoma. Cancer Discov 2014;4:1140–53.
31. Thota S, Kistangari G, Daw H, Spiro T. A clinical review of small-cell carcinoma of the urinary bladder. Clin Genitourin Cancer 2013;11:73–7.
32. Fine SW. Neuroendocrine lesions of the genitourinary tract. Adv Anat Pathol 2007;14:286–96.
33. Wick MR, Marchevsky AM. Neuroendocrine neoplasms of the lung: concepts and terminology. Semin Diagn Pathol 2015;32:445–55.
34. Watson PA, Arora VK, Sawyers CL. Emerging mechanisms of resistance to androgen receptor inhibitors in prostate cancer. Nat Rev Cancer 2015; 15:701–11.

AACR American Association for Cancer Research

Clinical Cancer Research

Small-Cell Carcinomas of the Bladder and Lung Are Characterized by a Convergent but Distinct Pathogenesis

Matthew T. Chang, Alexander Penson, Neil B. Desai, et al.

Clin Cancer Res 2018;24:1965-1973. Published OnlineFirst November 27, 2017.